

Tissue-Specific Regulation of Ferroportin in Wild-Type and *Hjv*^{-/-} Mice Following Dietary Iron Manipulations

Angeliki Katsarou,* Konstantinos Gkouvatso,*[#] Carine Fillebeen,* and Kostas Pantopoulos 

Hepcidin is a liver-derived peptide hormone that limits iron egress from tissues to the bloodstream. It operates by binding to the iron exporter ferroportin, which blocks iron transport and tags ferroportin for degradation. Genetic hepcidin inactivation leads to hereditary hemochromatosis, a disease of iron overload. We used wild-type and *Hjv*^{-/-} mice, a model of hemochromatosis, to examine the expression of ferroportin and other proteins of iron metabolism in hepcidin target tissues. The animals were previously subjected to dietary iron manipulations. In *Hjv*^{-/-} mice, hepcidin messenger RNA correlated significantly with hepatic iron load ($r = 0.8211$, $P < 0.001$), but was substantially lower compared with wild-type controls. Duodenal ferroportin and divalent metal transporter 1 (DMT1), as well as splenic and hepatic ferroportin, were overexpressed in these animals. A high-iron diet (2% carbonyl iron) suppressed duodenal DMT1 levels in both wild-type and *Hjv*^{-/-} mice; however, it did not affect duodenal ferroportin expression in *Hjv*^{-/-} mice, and only reduced it in wild-type mice. In contrast, the high-iron diet decreased splenic ferroportin exclusively in *Hjv*^{-/-} mice, whereas it induced hepatic ferroportin exclusively in wild-type mice. **Conclusion:** Our data show that dietary iron differentially affects ferroportin expression in mouse tissues and are consistent with hepcidin-dependent and hepcidin-independent mechanisms for ferroportin regulation. In the *Hjv*^{-/-} mouse model of hemochromatosis, duodenal ferroportin remains unresponsive to iron but DMT1 is appropriately iron-regulated. (*Hepatology Communications* 2021;5:2139-2150).

Hepcidin is a hormonal regulator of systemic iron homeostasis. It is secreted by hepatocytes and inhibits iron transport to the bloodstream.^(1,2) Hepcidin operates by binding to the iron exporter ferroportin, which occludes iron export⁽³⁾ and, moreover, triggers ferroportin ubiquitination and degradation.⁽⁴⁾ These responses limit dietary iron absorption by duodenal enterocytes, and the recycling of iron from phagocytized senescent erythrocytes by

tissue macrophages, primarily in the liver and spleen. Genetic defects in the hepcidin pathway promote increased iron absorption and lead to the development of systemic iron overload (hemochromatosis).^(5,6) The most common type of hereditary hemochromatosis is linked to mutations in the *HFE* gene encoding HFE, whereas rare variants are associated with mutations in the *TFR2*, *HJV*, or *HAMP* genes, encoding transferrin receptor 2 (TfR2), hemojuvelin (HJV) or hepcidin,

Abbreviations: ANOVA, analysis of variance; BMP, bone morphogenetic protein; DMT1, divalent metal transporter 1; *Hjv*, hemojuvelin; IRE, iron responsive element; mRNA, messenger RNA; PCR, polymerase chain reaction; SDS, sodium dodecyl sulfate; SMAD, mothers against decapentaplegic; TBS, Tris-buffered saline; Tf, transferrin; TfR1, transferrin receptor 1; Tris, tris(hydroxymethyl)aminomethane-buffered saline; wt, wild-type.

Received February 23, 2021; accepted June 17, 2021.

Additional Supporting Information may be found at onlinelibrary.wiley.com/doi/10.1002/hep4.1780/suppinfo.

*These authors contributed equally to this work.

Supported by the Canadian Institutes of Health Research (PJT-159730).

[#]Present address: Hôpital de Nyon, Chemin Monastier 10, 1260, Nyon, Switzerland.

© 2021 The Authors. *Hepatology Communications* published by Wiley Periodicals LLC on behalf of American Association for the Study of Liver Diseases. This is an open access article under the terms of the Creative Commons Attribution-NonCommercial-NoDerivs License, which permits use and distribution in any medium, provided the original work is properly cited, the use is non-commercial and no modifications or adaptations are made.

View this article online at [wileyonlinelibrary.com](https://onlinelibrary.wiley.com).

DOI 10.1002/hep4.1780

Potential conflict of interest: Nothing to report.

respectively. Iron overload varies among the hemochromatosis genotypes and correlates with the degree of hepcidin inactivation.

Hepcidin is induced transcriptionally primarily in response to iron or inflammatory signals; conversely, it is suppressed by iron deficiency or increased erythropoietic demand.^(1,2) Iron-dependent activation of the hepcidin pathway is mediated by bone morphogenetic protein (BMP)/mothers against decapentaplegic (SMAD) signaling, which involves phosphorylation of SMAD1/5/8, recruitment of SMAD4, and translocation of the complex to the nucleus for activation of the *HAMP* (hepcidin) promoter.⁽⁷⁾ It appears that increased transferrin (Tf) saturation is sensed by TfR2. On the other hand, elevated tissue iron stores promote secretion of BMP6 from liver sinusoidal endothelial cells, which in turn binds to BMP receptors and induces a potent SMAD response. BMP2 is likewise secreted from liver sinusoidal endothelial cells but is less responsive to iron and appears essential for basal hepcidin expression.

HJV is a BMP co-receptor and enhances basal and iron-dependent signaling to hepcidin. Pathogenic HJV mutations cause juvenile hemochromatosis, a disease characterized by early onset iron overload due to severe hepcidin deficiency.⁽⁸⁾ Ubiquitous^(9,10) or liver-specific^(11,12) *Hjv*^{-/-} mice recapitulate this phenotype. *Hjv*^{-/-} mice accumulate high levels of ferroportin in duodenal enterocytes and in macrophages of the spleen and the liver, as a result of hepcidin suppression.⁽¹⁰⁾ Nevertheless, they retain a limited capacity for hepcidin up-regulation by dietary iron.^(13,14)

We used wild-type and *Hjv*^{-/-} mice to address functional implications of intact and impaired hepcidin responses, respectively, to dietary iron manipulations. We analyzed expression of ferroportin and other iron proteins in tissues targeted by hepcidin. Our data

suggest that ferroportin is regulated by hepcidin-dependent and hepcidin-independent mechanisms in a tissue-specific manner.

Animals and Methods

ANIMALS

Wild-type and *Hjv*^{-/-} mice, both in C57BL/6 genetic background,⁽¹⁴⁾ were housed in macrolone cages (up to 5 mice/cage; 12-hour/12-hour light-dark cycle [7 AM to 7 PM]; 22° ± 1°C; 60% ± 5% humidity) according to standard institutional guidelines. Ten-week old male animals (n = 10 per each group) were placed on diets with variable iron content (Harlan Laboratories, Indianapolis, IN). The standard diet contained 225 ppm iron (2018 Teklad; Envigo, Indianapolis, IN). The low-iron diet contained 75–100 ppm iron (TD.05616), while the high-iron diet was the standard, enriched with 2% carbonyl iron (TD.09521). After 4 weeks, the mice were killed by cervical dislocation. Experimental procedures were approved by the Animal Care Committee of McGill University (protocol 4966).

SERUM BIOCHEMISTRY

Blood was collected with cardiac puncture. Serum was separated by centrifugation and used to determine iron concentration and Tf saturation by a Roche Hitachi 917 Chemistry Analyzer (Basel, Switzerland).

TISSUE IRON QUANTIFICATION

Tissue nonheme iron content was quantified by the ferrozine assay.⁽¹⁵⁾ Results are expressed as micrograms of iron per gram of dry tissue.

ARTICLE INFORMATION:

From the Department of Medicine, Lady Davis Institute for Medical Research, Jewish General Hospital, McGill University, Montreal, QC, Canada.

ADDRESS CORRESPONDENCE AND REPRINT REQUESTS TO:

Kostas Pantopoulos, Ph.D.
Department of Medicine, McGill University
Lady Davis Institute for Medical Research
Jewish General Hospital

3755 Cote-Ste-Catherine Road
Montreal, Quebec H3T 1E2, Canada
E-mail: kostas.pantopoulos@mcgill.ca
Tel.: +1-514-340-8260 ext. 25293

HISTOLOGICAL ANALYSIS

Tissue specimens from 3 animals per experimental group were fixed in 10% buffered formalin and embedded in paraffin. One section per animal was prepared for liver and spleen specimens, and three sections per animal for duodenal specimens. Samples were cut at 4 μ m, placed on SuperFrost/Plus slides (Thermo Fisher Scientific, Waltham, MA), and dried overnight at 37°C. The slides were then loaded onto the Discovery XT Autostainer (Ventana Medical Systems, Oro Valley, AZ) and underwent deparaffinization and heat-induced epitope retrieval for automated immunohistochemistry. Immunostaining was performed by using a 1:500 diluted custom-made ferroportin antibody⁽¹⁶⁾ and the Omnimap rabbit polyclonal horseradish peroxidase (#760-4311) detection kit.⁽¹⁷⁾ Slides were counterstained with hematoxylin, blued with Bluing Reagent, washed in warm soapy water, dehydrated through graded alcohols, cleared in xylene, and mounted with Permount (Thermo Fisher Scientific). Immunostained tissue slides were scanned using the Aperio ScanScope System (Leica BioSystems [Aperio], Vista, CA) at $\times 20$ or $\times 40$ magnifications, to provide high-resolution digital images. Slides with hematoxylin-stained splenic sections were analyzed and quantified for red and white pulp content by using the Aperio ImageScope software (Leica Biosystems).

WESTERN BLOTTING

The livers and spleens were washed with ice-cold phosphate-buffered saline (PBS) and dissected into pieces. Tissue aliquots were snap-frozen in liquid nitrogen and stored in a -80°C freezer. Duodenal segments were washed with ice-cold PBS and cut longitudinally. The mucosal layers were obtained by scraping with mild pressure using the short edge of a glass slide; subsequently, they were snap-frozen in liquid nitrogen and stored in a -80°C freezer. For western blot analysis, frozen tissue aliquots or mucosal scrapings were suspended in a lysis buffer containing 50 mM trishydroxymethylaminomethane (Tris)-Cl pH 8.0, 150 mM NaCl, 1% Triton X-100, 0.5% sodium deoxycholate, 0.1% sodium dodecyl sulfate (SDS), an ethylene diamine tetraacetic acid-free protease inhibitor cocktail (Roche) and a Halt phosphatase inhibitor Cocktail (Thermo Fisher Scientific). The suspensions were immediately homogenized with a TissueRuptor handheld homogenizer

(Qiagen, Hilden, Germany). Cell debris was cleared by centrifugation and the protein concentration was quantified with the DC-Protein Assay (Bio-Rad Laboratories, Hercules, CA). Lysates containing 40 μ g protein were resolved by SDS-polyacrylamide gel electrophoresis (PAGE) after boiling in a loading buffer containing 25 mM Tris-Cl pH 6.8, 2% SDS, 5% β -mercaptoethanol, 10% glycerol, and 0.0002% bromophenol blue. For detection of or liver ferroportin, we used 100 μ g of protein lysates. Ferroportin and DMT1 are transmembrane proteins prone to aggregation in response to heat or reducing agents; thus, the samples were not boiled before loading on the gel, and β -mercaptoethanol was omitted from the loading buffer. After termination of SDS-PAGE, the proteins were transferred from the polyacrylamide gel onto nitrocellulose filters. The blots were saturated with 10% nonfat milk in Tris-buffered saline buffered saline (TBS) containing 0.1% (vol/vol) Tween-20 (TBS-T) and probed with the following primary antibodies (all 1:1,000 diluted and raised in rabbit, unless otherwise indicated): custom-made ferroportin,⁽¹⁶⁾ custom-made DMT1,⁽¹⁸⁾ mouse monoclonal TfR1 (Zymed 13-6800, lot #VH307351), 1:500 diluted ferritin (NB600-920, lot #15656; Novus Biologicals, Littleton, CO), β -actin (A2066, lot #019M4777V; Sigma-Aldrich, St. Louis, MO), and villin (2369S; Cell Signaling Technology, Danvers, MA). After three washes with TBS-T, the blots were incubated with 1:20,000 goat anti-rabbit immunoglobulin G (IgG) (Jackson ImmunoResearch Laboratories, Inc., West Grove, PA) or 1:5,000 diluted peroxidase-coupled goat anti-mouse IgG (Jackson ImmunoResearch Laboratories). The peroxidase signal was visualized by enhanced chemiluminescence with the Western Lightning ECL kit (PerkinElmer, Waltham, MA). All original western blots are provided as supplemental material. Immunoreactive bands were quantified by densitometry with the ImageJ software and normalized to expression of β -actin. Densitometric data are represented as fold changes relative to samples from mice on standard diet.

QUANTITATIVE REAL-TIME POLYMERASE CHAIN REACTION

Total RNA was isolated from frozen tissues using the RNeasy Mini kit (Qiagen). Purity was assessed by 260/280 nm absorbance ratios, and quality was monitored by agarose gel electrophoresis. Complementary

DNA was synthesized from 1 μ g RNA by using the QuantiTect Reverse Transcription Kit (Qiagen). Quantitative real-time PCR was performed in a 7500 Fast Real Time PCR System (Applied Biosystems, Waltham, MA) with gene-specific primers provided in Supporting Table S1. Each primer pair was validated by dissociation curve analysis and demonstrated amplification efficiency between 90% and 110%. SYBR Green (Bioline AgroSciences, Essex, United Kingdom) and primers were used to amplify products under the following cycling conditions: initial denaturation at 95°C for 10 minutes, 40 cycles of 95°C for 5 seconds, 58°C for 30 seconds, 72°C for 10 seconds, and final cycle melt analysis between 58°C and 95°C. Relative messenger RNA (mRNA) expression was calculated by the comparative Ct method.⁽¹⁹⁾ Data normalized to β -actin or ribosomal protein L19 (Rpl19) are represented as fold changes to samples from wild-type mice on standard diet.

STATISTICS

Quantitative data were expressed as mean \pm SEM. The GraphPad Prism software (v. 7.0e) was used for statistical analysis with analysis of variance (ANOVA) and for Spearman rank correlation analysis. A probability value $P < 0.05$ was considered to be statistically significant.

Results

As expected, in wild-type mice fed with diets of variable iron content, hepcidin mRNA levels correlated significantly with both Tf saturation ($r = 0.5599$, $P < 0.05$) and hepatic iron levels ($r = 0.7772$, $P < 0.001$) (Fig. 1A,B). In *Hjv*^{-/-} mice, hepcidin mRNA levels were substantially lower and correlated significantly to hepatic iron load ($r = 0.8211$, $P < 0.001$), whereas Tf

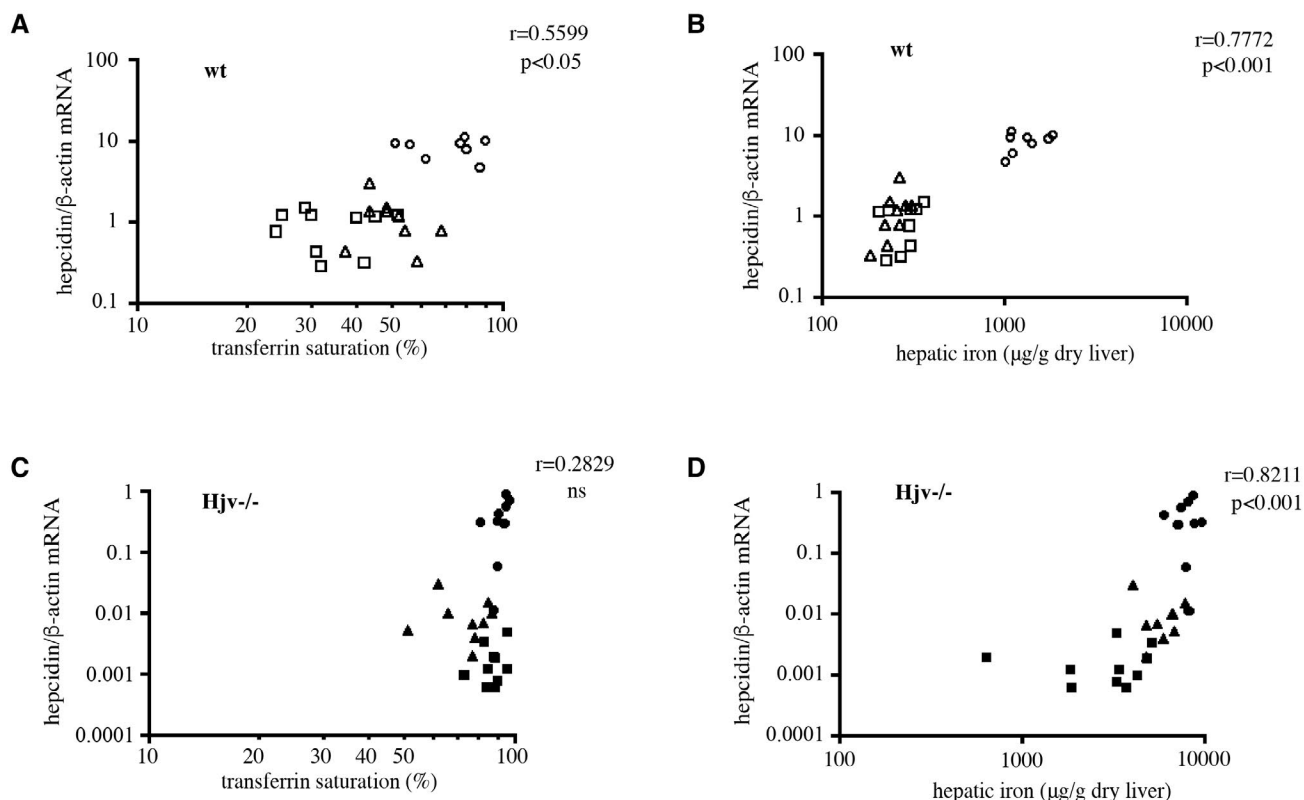


FIG. 1. Hepcidin mRNA levels correlate with hepatic iron load in *Hjv*^{-/-} mice subjected to dietary iron manipulations. Ten-week-old male *Hjv*^{-/-} and wild-type mice ($n = 10$ for each group) were fed for 4 weeks with diets of variable iron content (low: 75–100 ppm; standard: 225 ppm; high: 225 ppm plus 2% carbonyl iron). Hepcidin mRNA expression is plotted against Tf saturation (A,C) and hepatic iron content (B,D). Spearman's rank correlation analysis reveals a highly significant correlation of hepcidin mRNA with hepatic iron load of *Hjv*^{-/-} mice ($r = 0.8211$, $P < 0.001$). Squares represent low-iron diet; triangles represent standard-iron diet; and circles represent high-iron diet.

saturation reached a plateau under all dietary regimens (Fig. 1C,D). These findings confirm that *Hjv*^{-/-} mice can sense alterations in dietary iron levels and mount limited iron-dependent induction of hepcidin.^(13,14,20)

HIGH-IRON DIET SUPPRESSES SPLENIC FERROPORTIN IN *Hjv*^{-/-} BUT NOT WILD TYPE MICE

Ferroportin appears to be expressed at higher levels in splenic macrophages of *Hjv*^{-/-} versus

wild-type mice (Fig. 2A-C), in agreement with published data,^(10,17) and in spite of minor decreases in mRNA content (Fig. 2D). Western blot (Fig. 2A) and immunohistochemical data (Fig. 2C) show that high-iron diet did not significantly affect splenic ferroportin expression in wild-type mice, notwithstanding hepcidin induction (Fig. 1). Nevertheless, high-iron diet led to substantial and significant (2.8-fold, $P < 0.05$) reduction in splenic ferroportin content in *Hjv*^{-/-} mice (Fig. 2B), in line with their augmented iron-retaining capability in this

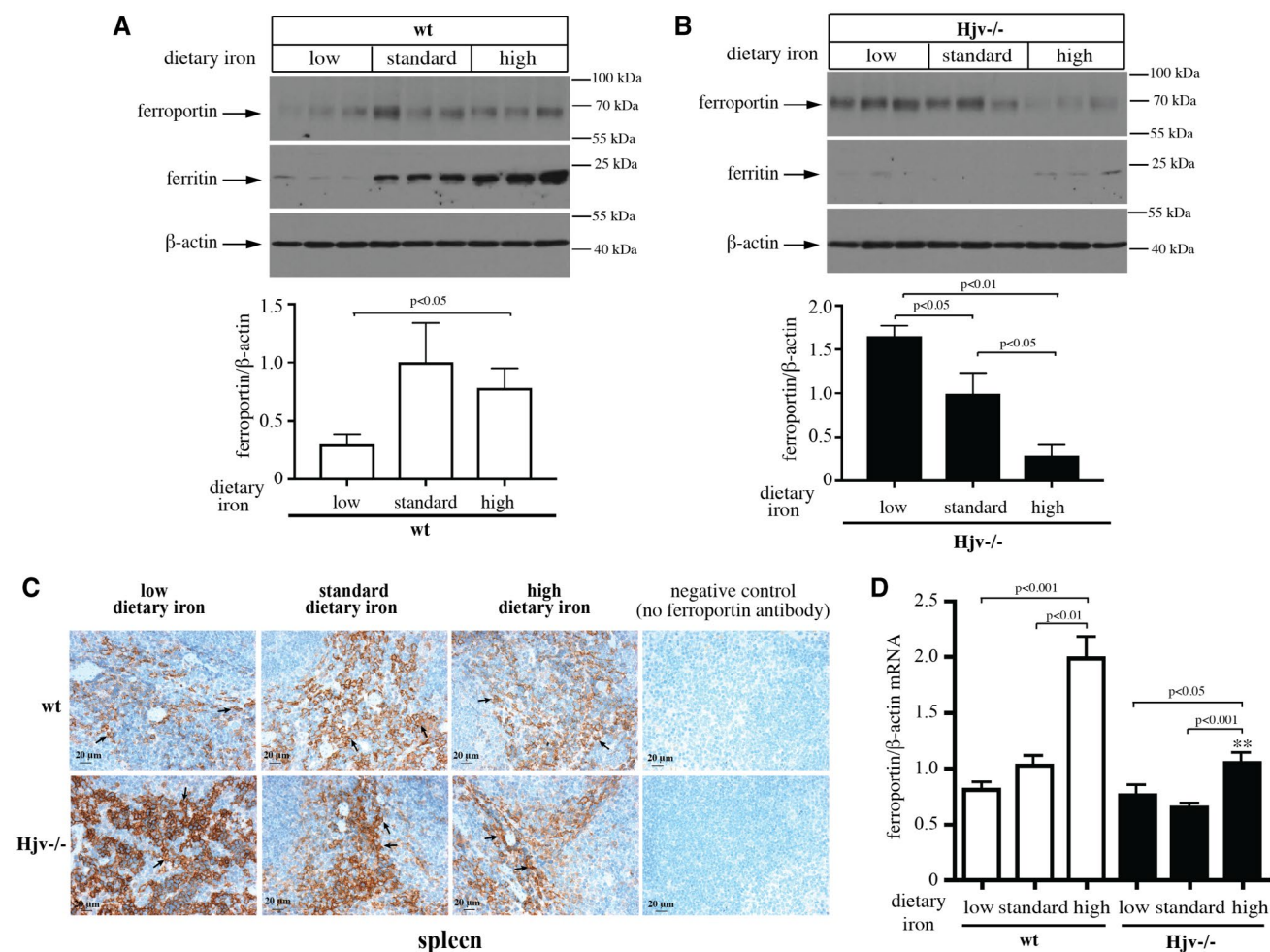


FIG. 2. Dietary iron loading down-regulates splenic ferroportin expression in *Hjv*^{-/-} but not wild-type mice. Splenic protein extracts, tissue sections, and RNA were prepared from the *Hjv*^{-/-} and wild-type mice described in Fig. 1 and used for western blotting, immunohistochemistry, and quantitative real-time PCR, respectively. (A,B) Analysis of ferroportin, ferritin, and control β -actin expression in representative samples from each group ($n = 3$) of wild-type (A) and *Hjv*^{-/-} (B) mice. Densitometric quantification of ferroportin/ β -actin (corresponding to $n = 6$ mice for each group) is shown below the western panels. (C) Immunohistochemical detection of splenic ferroportin (original magnification: $\times 20$). Representative ferroportin-expressing cells are indicated by arrows. (D) Analysis of splenic ferroportin mRNA ($n = 10$ for each group). All quantitative data are presented as the mean \pm SEM. Statistical analysis was performed by two-way ANOVA. Statistically significant differences across genotypes in (D) are indicated by $**P < 0.01$. Abbreviation: wt, wild-type.

organ under similar experimental conditions.^(14,20) These responses were associated with significant increases in ferroportin mRNA (1.4-fold, $P < 0.001$ in *Hjv*^{-/-} mice; and 2-fold, $P < 0.01$ in wild-type mice, respectively) (Fig. 2D). Interestingly, low-iron diet diminished splenic ferroportin content in wild-type mice (Fig. 2A) but elicited opposite effects in *Hjv*^{-/-} animals (Fig. 2B). Ferritin levels (Fig. 2A, second panel) corroborated splenic iron load in wild-type mice but were close to detection limit in *Hjv*^{-/-} mice (Fig. 2B, second panel). We did not observe any differences in cellularity of the spleen between

wild-type and *Hjv*^{-/-} mice under all dietary regimens (Supporting Fig. S1).

HIGH-IRON DIET STIMULATES LIVER FERROPORTIN EXPRESSION IN WILD-TYPE BUT NOT *Hjv*^{-/-} MICE

Immunohistochemical analysis of liver sections showed robust expression of ferroportin in Kupffer cells, with apparently stronger signal intensity in *Hjv*^{-/-} mice (Fig. 3A, arrows). The staining was predominant

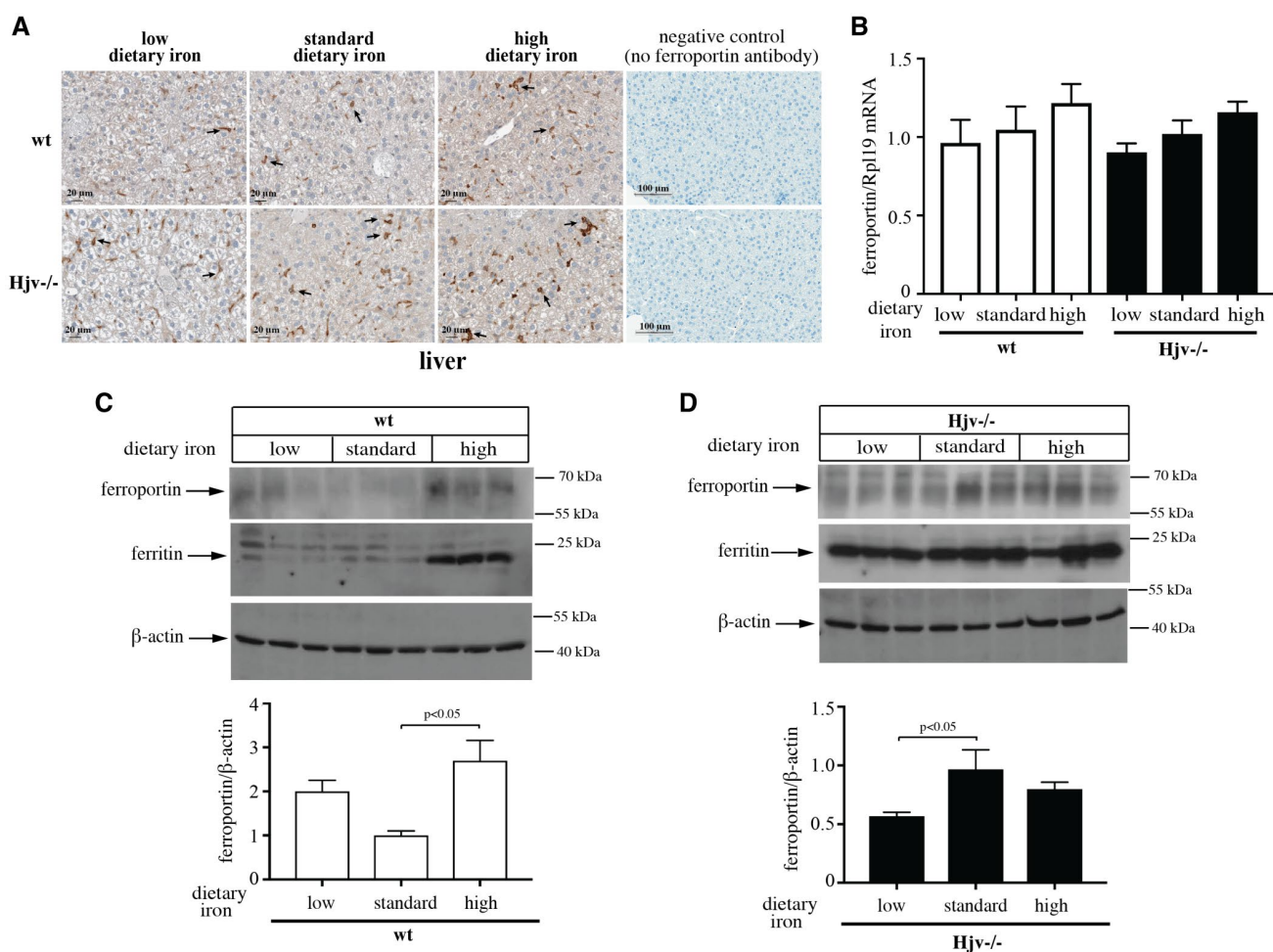


FIG. 3. Dietary iron loading stimulates liver ferroportin expression in wild type but not *Hjv*^{-/-} mice. Liver protein extracts, tissue sections and RNA were prepared from the *Hjv*^{-/-} and wild type mice described in Fig. 1 and used for immunohistochemistry, qPCR and Western blotting, respectively. (A) Immunohistochemical detection of ferroportin in liver sections (original magnification: 20x). Representative ferroportin-expressing cells are indicated by arrows. (B) Analysis of liver ferroportin mRNA ($n = 10$ for each group). (C and D) Analysis of ferroportin, ferritin and control β -actin expression in representative samples from each group ($n = 3$) of wild type (C) and *Hjv*^{-/-} (D) mice. Densitometric quantification of ferroportin/ β -actin (corresponding to $n = 6$ mice for each group) is shown below the Western panels. All quantitative data are presented as the mean \pm SEM. Statistical analysis was performed by two-way ANOVA.

in periportal areas (Fig. S2). Hepatocellular ferroportin expression was also evident in *Hjv*^{-/-} livers, and especially in hepatocytes around portal triads (Supporting Fig. S2). However, the signal was weaker compared with that in Kupffer cells, while slight variations were noted among samples (not shown). Western blot analysis shows that the high-iron diet induced significantly ($P < 0.05$) total liver ferroportin expression in wild-type (Fig. 3C) but not *Hjv*^{-/-} mice (Fig. 3D). Nevertheless, a more intense ferroportin staining in Kupffer cells was evident in both genotypes after high dietary iron intake (Fig. 3A). The low-iron diet did not affect liver ferroportin expression in wild-type mice, but slightly reduced it in *Hjv*^{-/-} animals. As expected, ferritin content was augmented in the liver of iron-loaded wild-type mice and remained elevated in the liver of all *Hjv*^{-/-} mice independently of dietary regimen (Fig. 3C,3D). Liver ferroportin mRNA levels did not significantly differ among the genotypes and did not change in response to diets (Fig. 3B).

BOTH WILD-TYPE AND *Hjv*^{-/-} MICE SUPPRESS DUODENAL DMT1, BUT ONLY THE FORMER INHIBIT DUODENAL FERROPORTIN EXPRESSION IN RESPONSE TO HIGH-IRON DIET

DMT1 is expressed on the apical membrane of enterocytes⁽²¹⁾ and mediates dietary iron absorption from the intestinal lumen.⁽²²⁾ Duodenal extracts from *Hjv*^{-/-} mice appeared to contain considerably higher DMT1 levels compared with wild-type controls (Fig. 4A,B, upper panel). Purity of the duodenal extract preparation is indicated by the presence of villin, a marker of brush border enterocytes.⁽²³⁾ Importantly, duodenal DMT1 was strongly induced in *Hjv*^{-/-} mice on low-iron diet and, conversely, dramatically inhibited in mice fed with high-iron diet (Fig. 4B). Induction of DMT1 was also observed in iron-poor wild-type controls, whereas dietary iron loading appeared to further reduce DMT1 content (Fig. 4A). These effects were associated with alterations in DMT1 mRNA. Thus, *Hjv*^{-/-} mice exhibited 6-fold ($P < 0.01$) higher expression of duodenal DMT1 mRNA compared with wild-type controls on standard diet (Fig. 5C). DMT1 mRNA levels were increased by the low-iron diet (2.4-fold, $P < 0.05$ in

Hjv^{-/-} mice; and 2-fold, $P < 0.05$ in wild type mice, respectively) and reduced by the iron-enriched diet in *Hjv*^{-/-} mice (2.9-fold, $P < 0.05$). These results highlight an important role of DMT1 in the development of iron overload in *Hjv*^{-/-} mice. In addition, they suggest that the iron-dependent regulation of DMT1 largely operates at the transcript level.

Ferroportin was markedly induced in the duodenum of *Hjv*^{-/-} versus wild-type mice (Figs. 4 and 5A), in agreement with previous findings.^(10,11) In animals on standard diet, this was associated with moderate (0.7-fold) but significant ($P < 0.05$) up-regulation of ferroportin mRNA (Fig. 5B). In wild-type animals, duodenal ferroportin decreased by the high-iron diet and, conversely, increased by the low-iron diet (Fig. 4A); the latter was associated with a significant ($P < 0.05$) 2-fold mRNA induction (Fig. 5B). In contrast, duodenal ferroportin did not respond to dietary iron alterations in *Hjv*^{-/-} mice (Fig. 4B), whereas the induction of its mRNA by the lower iron diet was preserved (Fig. 5B). The immunohistochemical analysis in Fig. 5A validates the western blot data. Taken together, the findings in Figs. 2-5 highlight tissue-specific differences in the regulation of splenic, hepatic, and duodenal ferroportin, and demonstrate a failure of *Hjv*^{-/-} mice to mount appropriate tissue ferroportin responses to high-iron diet.

TfR1 is expressed on the basolateral membrane of intestinal crypt cells and mediates uptake of Tf-bound iron from the bloodstream.⁽²⁴⁾ TfR1 and ferritin are coordinately and reciprocally regulated post-transcriptionally by the “iron-responsive element/iron regulatory protein” system.⁽²⁵⁾ Western blot analysis shows the expected pattern of duodenal TfR1 and ferritin expression in both wild-type and *Hjv*^{-/-} mice (Fig. 4A,B; quantification of the western blots is shown in Supporting Fig. S3). The apparently higher TfR1 and lower ferritin levels in the *Hjv*^{-/-} duodenum may reflect the known iron deficiency of this tissue in hereditary hemochromatosis.⁽²⁶⁾ Importantly, the high-iron diet triggered a noticeable induction of duodenal ferritin in *Hjv*^{-/-} mice, which indicates iron retention. Indeed, quantification revealed a significant ($P < 0.01$) 0.6-fold increase in duodenal iron content under these conditions (Fig. 5D). Thus, high-iron diet promotes at least partial duodenal iron retention in *Hjv*^{-/-} mice, in spite of the maintenance of pathological ferroportin levels.

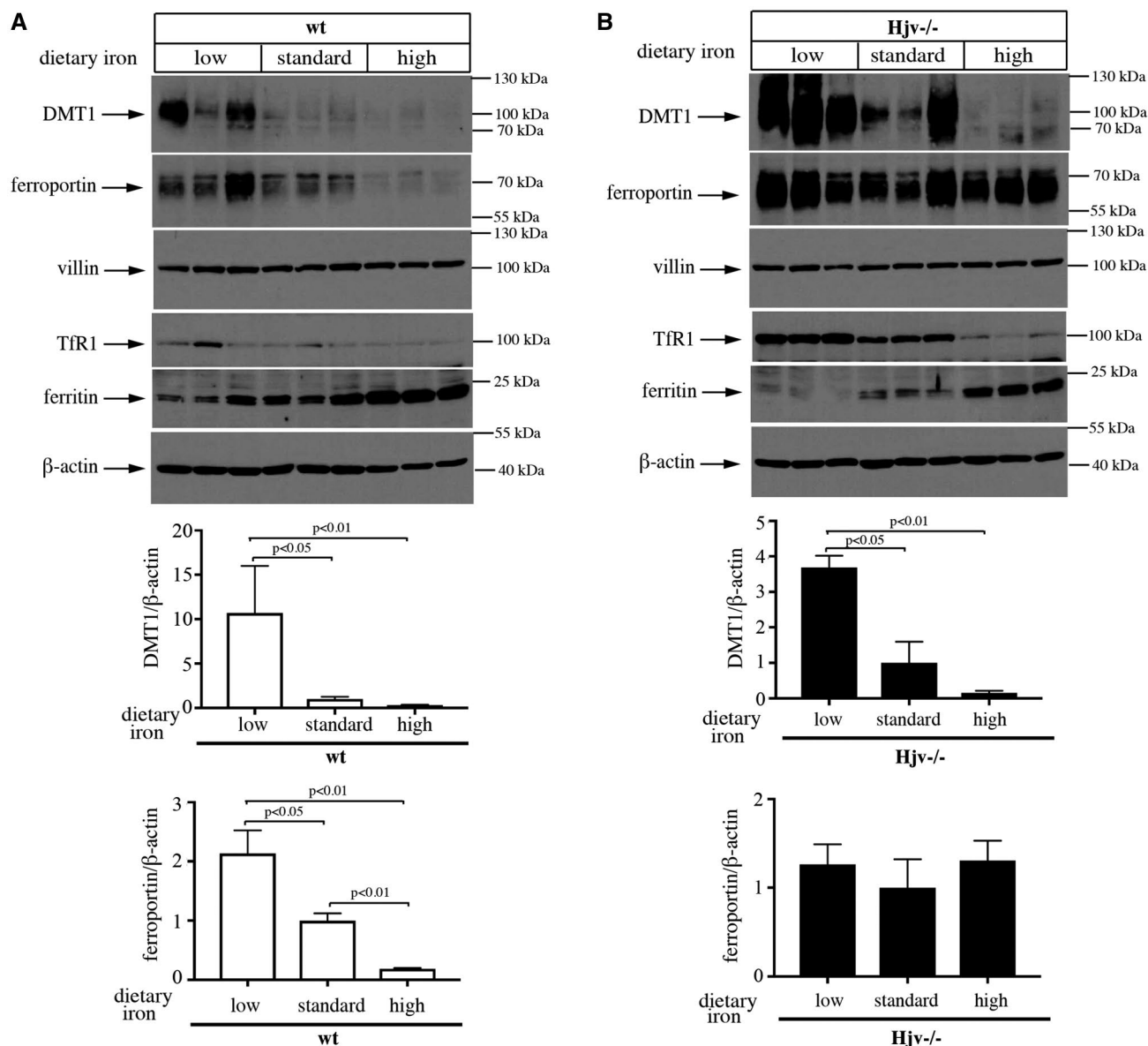


FIG. 4. Differential expression and iron-dependent regulation of duodenal DMT1 and ferroportin in wild-type and *Hjv*^{-/-} mice. Duodenal mucosal lysates were prepared from *Hjv*^{-/-} and wild-type mice described in Fig. 1 and used for western blotting. (A,B) Expression of DMT1, ferroportin, TfR1, villin, ferritin, and β -actin in representative samples from each group ($n = 3$) of wild-type (A) and *Hjv*^{-/-} (B) mice. Densitometric quantification of DMT1/ β -actin and ferroportin/ β -actin (corresponding to $n = 6$ mice for each group) is shown below the western panels; quantification of TfR1/ β -actin and ferritin/ β -actin is shown separately in Supporting Fig. S3. All quantitative data are presented as the mean \pm SEM. Statistical analysis was performed by two-way ANOVA.

Discussion

We show that wild-type and *Hjv*^{-/-} mice differentially regulate ferroportin expression in major iron-exporting tissues in response to dietary iron manipulations. *Hjv*^{-/-} mice express higher ferroportin levels in the spleen, liver, and duodenum compared

with age-matched and gender-matched isogenic wild types, as a result of severe genetic inactivation of hepcidin. We previously demonstrated that these animals retain a capacity for regulating residual hepcidin in response to iron^(14,20) but also to inflammatory signals.⁽¹⁷⁾ The data in Fig. 1 corroborate the published data and, furthermore, raise the possibility that

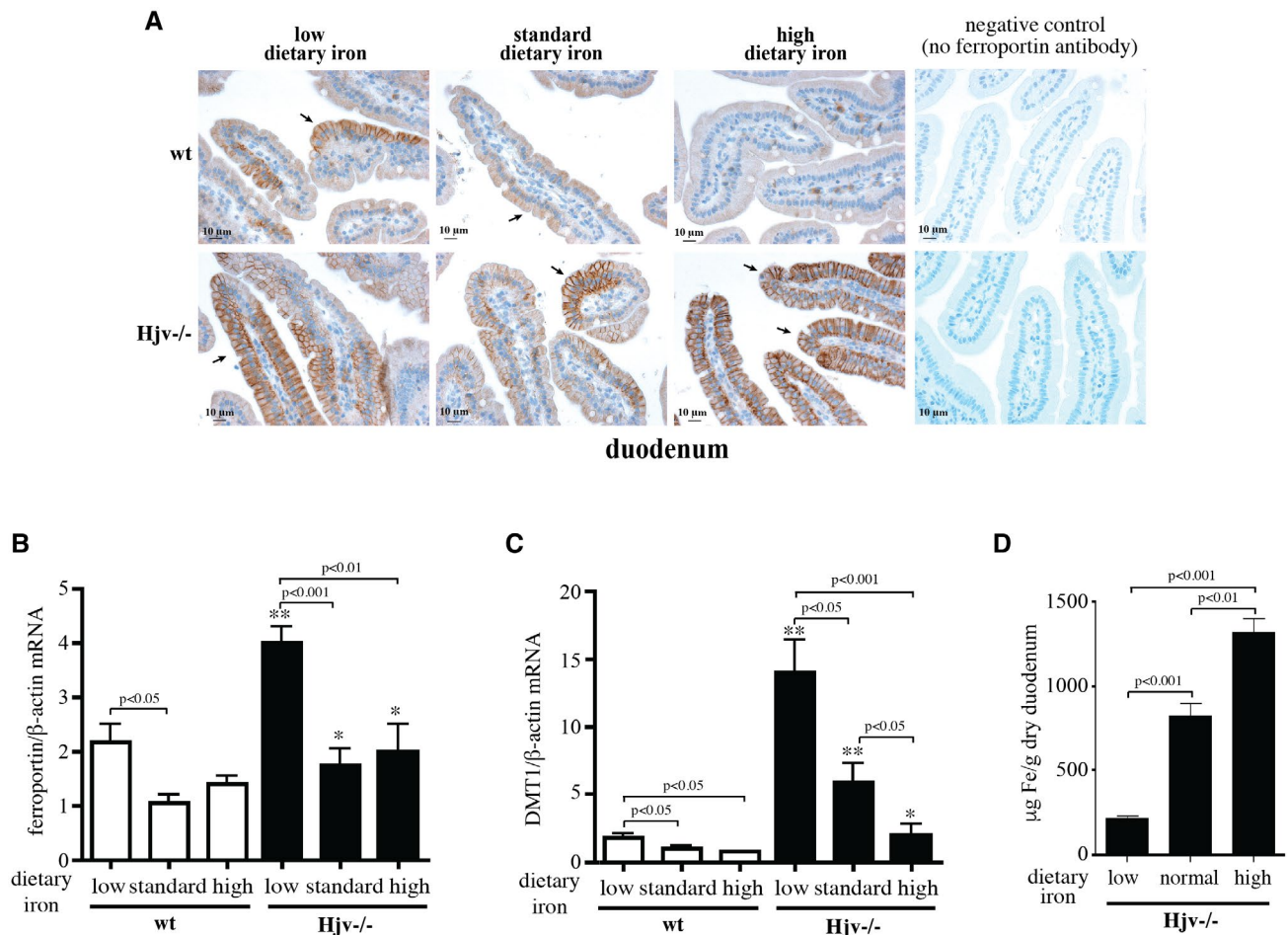


FIG. 5. Immunohistochemical detection of duodenal ferroportin and analysis of duodenal ferroportin and DMT1 mRNAs and iron content. Duodenal sections, RNA, and tissue segments were prepared from Hjv^{-/-} and wild-type mice described in Fig. 1 and used for immunohistochemistry, quantitative real-time PCR, and iron quantification, respectively. (A) Immunolocalization of ferroportin (original magnification: $\times 40$). Representative ferroportin-expressing cells are indicated by arrows. (B) Analysis of ferroportin mRNA ($n = 10$ for each group). (C) Analysis of DMT1 mRNA ($n = 10$ for each group). (D) High-iron diet promotes partial duodenal iron retention in Hjv^{-/-} mice. Duodenal segments from the Hjv^{-/-} mice described in Fig. 1 were isolated and used for quantification of nonheme iron by the ferrozine assay ($n = 10$ for each group). Data are presented as the mean \pm SEM. Statistical analysis was performed by one-way ANOVA. Statistically significant differences across genotypes in (B) and (C) are indicated by * $P < 0.05$ or ** $P < 0.01$.

iron-dependent induction of residual hepcidin may account for the decreased ferroportin content in the spleens of Hjv^{-/-} mice on high-iron diet (Fig. 2B). A contribution of splenic hepcidin cannot be formally excluded but is unlikely because its levels are minuscule.⁽¹⁴⁾

In spleens of wild-type mice, ferroportin was not significantly reduced following a high-iron diet, even though a trend was apparent (Fig. 2A). We speculate that hepcidin-dependent degradation of splenic ferroportin may be counterbalanced by translational de-repression of its mRNA, which contains

a “translation-type” IRE and is highly expressed in iron-replete conditions.⁽²⁷⁾ The induction of ferroportin mRNA (Fig. 2D), possibly through transcriptional mechanisms,^(28,29) would further augment this response. Conversely, suppression of ferroportin mRNA translation would explain the decrease in ferroportin steady-state levels observed in wild-type mice on low-iron diet. Presumably, splenic ferroportin mRNA is likewise poorly translated in Hjv^{-/-} mice. The reason is that macrophages fail to retain iron in hemochromatosis, and, consequently, the spleen becomes iron-deficient. Nevertheless, the dramatic

suppression of hepcidin in *Hjv*^{-/-} mice may allow unrestricted accumulation of even inefficiently synthesized protein.

Ferroportin is expressed in red pulp macrophages of the spleen; in fact, we have shown that the ferroportin signal co-localizes with the macrophage marker *c-fms* in immunohistochemical experiments.⁽¹⁷⁾ On the other hand, liver ferroportin is expressed in macrophages (Kupffer cells),⁽¹⁷⁾ as well as in parenchymal cells (hepatocytes).⁽³⁰⁾ Hepatocellular ferroportin is not always detectable by immunohistochemistry but very likely contributes to the apparent increase in biochemically detectable liver ferroportin content in *Hjv*^{-/-} mice compared with controls (Fig. 3). Presumably, hepatocellular ferroportin also accounts for the increase in liver ferroportin content in wild-type mice on a high-iron diet. In light of the strong up-regulation of hepcidin under these conditions (Fig. 1), this response appears counterintuitive. Nonetheless, by analogy to a similar but less pronounced effect observed in the spleen (Fig. 2), the ferroportin-degrading action of hepcidin may be negated by increased ferroportin synthesis due to translational de-repression of its mRNA. It is also conceivable that hepcidin remains operational by occluding iron efflux from ferroportin under these conditions. This interpretation is supported by the induction of ferritin, which is indicative of cellular iron retention and overload.

Liver sections from *Hjv*^{-/-} mice exhibit more intense ferroportin staining in Kupffer cells compared with wild-type controls (Fig. 3), which is a result of hepcidin deficiency.⁽¹⁰⁾ The intensity of the staining tends to increase in response to high-iron diet, even though the overall ferroportin content remains unchanged. This may reflect increased ferroportin synthesis in Kupffer cells, assuming that they can retain some iron by analogy to splenic macrophages under similar experimental conditions.^(14,20) We speculate that the increased ferroportin expression in Kupffer cells does not lead to an overall increase in liver ferroportin content because of a “dilution effect” in more abundant and highly expressed hepatocellular ferroportin. Liver ferroportin mRNA levels remained unresponsive to dietary iron manipulations in both wild-type and *Hjv*^{-/-} mice, highlighting that iron-dependent ferroportin expression in this organ is regulated by post-transcriptional mechanisms.

In the duodenum, ferroportin is expressed on the basolateral membrane of enterocytes.⁽³¹⁾ In wild-type

mice, duodenal ferroportin is appropriately suppressed by high-iron and induced by low-iron diets, respectively (Fig. 4A). These responses are consistent with hepcidin regulation. Moreover, the increased ferroportin mRNA levels in the duodenum of wild-type mice fed iron-poor diet is in line with transcriptional induction through hypoxia inducible factor 2 α (HIF-2 α).⁽³²⁾ Because duodenal ferroportin is encoded by an alternatively spliced transcript that lacks an iron-responsive element,⁽²⁷⁾ iron loading is not expected to stimulate its translation.

Although residual iron-dependent induction of hepcidin in *Hjv*^{-/-} mice may have functional implications in the spleen, it clearly does not affect duodenal ferroportin levels (Fig. 4B). This may indicate tissue-specific differences in ferroportin regulation by hepcidin, as proposed in previous studies.^(33,34) However, it is also possible that duodenal ferroportin requires a higher threshold of hepcidin to undergo degradation. In this case, its high expression in *Hjv*^{-/-} mice on high-iron diet would indicate hepcidin insufficiency. On the other hand, the increased duodenal iron retention in *Hjv*^{-/-} on a high-iron diet (Fig. 5D) may suggest that up-regulated residual hepcidin in these animals operates by occluding iron efflux. Pharmacological experiments with synthetic hepcidin or analogues can shed light on the responsiveness of overexpressed duodenal ferroportin to hepcidin and the underlying mechanisms.

The data in Fig. 4 show that duodenal DMT1 is also overexpressed in *Hjv*^{-/-} mice and, furthermore, it is profoundly suppressed by iron. Previous reports identified increased duodenal DMT1 mRNA expression in *Hfe*^{-/-} mice⁽³⁵⁾ as well as in patients with HFE hemochromatosis,⁽³⁶⁾ suggesting an important contribution of this transporter in the development of genetic iron overload. Nevertheless, DMT1 mRNA and protein levels were physiological in another *Hfe*^{-/-} mouse strain, and it was argued that the augmentation of DMT1 mRNA in patients may be a secondary effect to therapeutic phlebotomies.⁽³⁷⁾ Our results are in agreement with the increased DMT1 expression seen in *Hamp*^{-/-} mice,⁽³⁸⁾ an additional model of juvenile hemochromatosis, and indicate that duodenal DMT1 levels correlate with the degree of systemic iron overload and intestinal iron deficiency.

Duodenal DMT1 is subjected to iron regulation by transcriptional and post-transcriptional mechanisms.⁽³⁹⁾ Thus, under iron deficiency, its mRNA is

transcriptionally activated by HIF-2 α ,⁽³²⁾ whereas IRE-containing isoforms are post-transcriptionally stabilized by iron regulatory proteins.⁽²⁵⁾ Our DMT1 mRNA analysis (Fig. 5C) is consistent with both scenarios. At the protein level, duodenal DMT1 has been proposed to be an additional molecular target of hepcidin,⁽³⁴⁾ but it is unclear whether circulating hepcidin can reach DMT1, which is expressed on the apical membrane of duodenal enterocytes. We speculate that the suppression of duodenal DMT1 in HJV^{-/-} mice on high-iron diet is driven by the relatively increased duodenal iron content in these animals. The possibility that residual hepcidin contributes to this effect is intriguing but requires experimental validation.

In conclusion, our data suggest that ferroportin expression is iron-regulated by hepcidin-dependent and hepcidin-independent mechanisms in iron-exporting mouse tissues. Understanding these mechanisms is critical in the context of pharmacological targeting of hepcidin pathways for the treatment of iron overload disorders. Moreover, duodenal DMT1 may offer another legitimate pharmacological target against hemochromatosis.

Acknowledgment: The authors thank Dr. Naciba Benlimame and Lilian Canetti for assistance with the histology.

REFERENCES

- 1) Katsarou A, Pantopoulos K. Basics and principles of cellular and systemic iron homeostasis. *Mol Aspects Med* 2020;75:100866.
- 2) Muckenthaler MU, Rivella S, Hentze MW, Galy B. A red carpet for iron metabolism. *Cell* 2017;168:344-361.
- 3) **Billesbølle CB, Azumaya CM, Kretsch RC, Powers AS, Gonen S, Schneider S, et al.** Structure of hepcidin-bound ferroportin reveals iron homeostatic mechanisms. *Nature* 2020;586:807-811.
- 4) Qiao B, Sugianto P, Fung E, Del-Castillo-Rueda A, Moran-Jimenez MJ, Ganz T, et al. Hepcidin-induced endocytosis of ferroportin is dependent on ferroportin ubiquitination. *Cell Metab* 2012;15:918-924.
- 5) Pantopoulos K. Inherited disorders of iron overload. *Front Nutrition* 2018;5:103.
- 6) Camaschella C, Nai A, Silvestri L. Iron metabolism and iron disorders revisited in the hepcidin era. *Haematologica* 2020;105:260-272.
- 7) Wang CY, Babitt JL. Liver iron sensing and body iron homeostasis. *Blood* 2019;133:18-29.
- 8) Papanikolaou G, Samuels ME, Ludwig EH, MacDonald ML, Franchini PL, Dube MP, et al. Mutations in HFE2 cause iron overload in chromosome 1q-linked juvenile hemochromatosis. *Nat Genet* 2004;36:77-82.
- 9) **Niederkofer V, Salie R, Arber S.** Hemojuvelin is essential for dietary iron sensing, and its mutation leads to severe iron overload. *J Clin Invest* 2005;115:2180-2186.
- 10) Huang FW, Pinkus JL, Pinkus GS, Fleming MD, Andrews NC. A mouse model of juvenile hemochromatosis. *J Clin Invest* 2005;115:2187-2191.
- 11) Gkouvatso K, Wagner J, Papanikolaou G, Sebastiani G, Pantopoulos K. Conditional disruption of mouse Hfe2 gene: maintenance of systemic iron homeostasis requires hepatic but not skeletal muscle hemojuvelin. *Hepatology* 2011;54:1800-1807.
- 12) Chen W, Huang FW, de Renshaw TB, Andrews NC. Skeletal muscle hemojuvelin is dispensable for systemic iron homeostasis. *Blood* 2011;117:6319-6325.
- 13) Ramos E, Kautz L, Rodriguez R, Hansen M, Gabayan V, Ginzburg Y, et al. Evidence for distinct pathways of hepcidin regulation by acute and chronic iron loading in mice. *Hepatology* 2011;53:1333-1341.
- 14) **Gkouvatso K, Fillebeen C, Daba A, Wagner J, Sebastiani G, Pantopoulos K.** Iron-dependent regulation of hepcidin in HJV^{-/-} mice: evidence that hemojuvelin is dispensable for sensing body iron levels. *PLoS One* 2014;9:e85530.
- 15) Daba A, Gkouvatso K, Sebastiani G, Pantopoulos K. Differences in activation of mouse hepcidin by dietary iron and parenterally administered iron dextran: compartmentalization is critical for iron sensing. *J Mol Med (Berl)* 2013;91:95-102.
- 16) Maffettone C, Chen G, Drozdov I, Ouzounis C, Pantopoulos K. Tumorigenic properties of iron regulatory protein 2 (IRP2) mediated by its specific 73-amino acids insert. *PLoS One* 2010;5:e10163.
- 17) **Fillebeen C, Wilkinson N, Charlebois E, Katsarou A, Wagner J, Pantopoulos K.** Hepcidin-mediated hypoferremic response to acute inflammation requires a threshold of Bmp6/HJV/Smad signaling. *Blood* 2018;132:1829-1841.
- 18) Schümann K, Herbach N, Kerling C, Seifert M, Fillebeen C, Prysck I, et al. Iron absorption and distribution in TNFAARE/+ mice, a model of chronic inflammation. *J Trace Elem Med Biol* 2010;24:58-66.
- 19) Livak KJ, Schmittgen TD. Analysis of relative gene expression data using real-time quantitative PCR and the 2(-Delta Delta C(T)) method. *Methods* 2001;25:402-408.
- 20) Kent P, Wilkinson N, Constante M, Fillebeen C, Gkouvatso K, Wagner J, et al. Hfe and HJV exhibit overlapping functions for iron signaling to hepcidin. *J Mol Med (Berl)* 2015;93:489-498.
- 21) Canonne-Hergaux F, Gruenheid S, Ponka P, Gros P. Cellular and subcellular localization of the Nramp2 iron transporter in the intestinal brush border and regulation by dietary iron. *Blood* 1999;93:4406-4417.
- 22) Gunshin H, Mackenzie B, Berger UV, Gunshin Y, Romero MF, Boron WF, et al. Cloning and characterization of a mammalian protein-coupled metal-ion transporter. *Nature* 1997;388:482-488.
- 23) Bretscher A, Weber K. Villin is a major protein of the microvillus cytoskeleton which binds both G and F actin in a calcium-dependent manner. *Cell* 1980;20:839-847.
- 24) Waheed A, Parkkila S, Saarnio J, Fleming RE, Zhou XY, Tomatsu S, et al. Association of HFE protein with transferrin receptor in crypt enterocytes of human duodenum. *Proc Natl Acad Sci USA* 1999;96:1579-1584.
- 25) Wilkinson N, Pantopoulos K. The IRP/IRE system in vivo: insights from mouse models. *Front Pharmacol* 2014;5:176.
- 26) Pietrangelo A, Casalgrandi G, Quagliano D, Gualdi R, Conte D, Milani S, et al. Duodenal ferritin synthesis in genetic hemochromatosis. *Gastroenterology* 1995;108:208-217.
- 27) Zhang DL, Hughes RM, Ollivierre-Wilson H, Ghosh MC, Rouault TA. A ferroportin transcript that lacks an iron-responsive element enables duodenal and erythroid precursor cells to evade translational repression. *Cell Metab* 2009;9:461-473.
- 28) **Zoller H, Theurl I, Koch R, Kaser A, Weiss G.** Mechanisms of iron mediated regulation of the duodenal iron transporters divalent metal transporter 1 and ferroportin 1. *Blood Cells Mol Dis* 2002;29:488-497.

- 29) Brewer CJ, Wood RI, Wood JC. mRNA regulation of cardiac iron transporters and ferritin subunits in a mouse model of iron overload. *Exp Hematol* 2014;42:1059-1067.
- 30) Ramey G, Deschemin JC, Durel B, Canonne-Hergaux F, Nicolas G, Vaulont S. Heparin targets ferroportin for degradation in hepatocytes. *Haematologica* 2010;95:501-504.
- 31) Donovan A, Brownlie A, Zhou YI, Shepard J, Pratt SJ, Moynihan J, et al. Positional cloning of zebrafish ferroportin1 identifies a conserved vertebrate iron exporter. *Nature* 2000;403:776-781.
- 32) Schwartz AJ, Das NK, Ramakrishnan SK, Jain C, Jurkovic MT, Wu J, et al. Hepatic hepcidin/intestinal HIF-2alpha axis maintains iron absorption during iron deficiency and overload. *J Clin Invest* 2019;129:336-348.
- 33) Chaston T, Chung B, Mascarenhas M, Marks J, Patel B, Srini SK, et al. Evidence for differential effects of hepcidin in macrophages and intestinal epithelial cells. *Gut* 2008;57:374-382.
- 34) Brasse-Lagnel C, Karim Z, Letteron P, Bekri S, Bado A, Beaumont C. Intestinal DMT1 cotransporter is down-regulated by hepcidin via proteasome internalization and degradation. *Gastroenterology* 2011;140:1261-1271.e1261.
- 35) Fleming RE, Migas MC, Zhou X, Jiang J, Britton RS, Brunt EM, et al. Mechanism of increased iron absorption in murine model of hereditary hemochromatosis: increased duodenal expression of the iron transporter DMT1. *Proc Natl Acad Sci USA* 1999;96:3143-3148.
- 36) Zoller H, Pietrangelo A, Vogel W, Weiss G. Duodenal metal-transporter (DMT-1, NRAMP-2) expression in patients with hereditary haemochromatosis. *Lancet* 1999;353:2120-2123.
- 37) Canonne-Hergaux F, Levy JE, Fleming MD, Montross LK, Andrews NC, Gros P. Expression of the DMT1 (NRAMP2/DCT1) iron transporter in mice with genetic iron overload disorders. *Blood* 2001;97:1138-1140.
- 38) Viatte L, Lesbordes-Brion J-C, Lou D-Q, Bennoun M, Nicolas G, Kahn A, et al. Deregulation of proteins involved in iron metabolism in hepcidin-deficient mice. *Blood* 2005;105:4861-4864.
- 39) Tchernitchko D, Bourgeois M, Martin ME, Beaumont C. Expression of the two mRNA isoforms of the iron transporter Nramp2/DMT1 in mice and function of the iron responsive element. *Biochem J* 2002;363:449-455.

Author names in bold designate shared co-first authorship.

Supporting Information

Additional Supporting Information may be found at onlinelibrary.wiley.com/doi/10.1002/hep4.1780/supinfo.